DOI 10.1007/s11015-021-01161-6
Metallurgist, Vol. 65, Nos. 3-4, July, 2021 (Russian Original Nos. 3-4, March–April, 2021)

RELATIONSHIP BETWEEN MECHANICAL PROPERTIES AND NATURE OF FRACTURE SURFACE OF POWDER STEELS UNDER HIGH-TEMPERATURE TENSION

M. S. Egorov[1] **and R. V. Egorova**[2]

UDC 621.762.1

Results of research on high-temperature tension for powder steels by the Swedish company Höganäs are analyzed. Morphological differences in the structure through the cross-section of a cylindrical specimen, which is conventionally divided into central and peripheral areas, are revealed. Microstructural analysis and fractographic study of the fracture surface are performed in each area. These studies provide identification of areas of fractures having different relief in intercrystalline shears and their extent, which indicates the presence of areas on the surface of interparticle contact with different degrees of completion of interparticle fusion. It is shown that plastic flow is accompanied by formation of peripheral region material whose structure and properties depend on the degree of deformation and production conditions. As the peripheral region develops material strength properties decrease after reaching a critical amount of transverse flow. Mechanical properties of specimens prepared from the highest quality materials are studied in detail at high temperature. This provides a complete picture of the occurrence of microcracks and the potential for using the material under actual conditions.

Keywords: high-temperature tension, ultimate strength, yield strength, elongation, surface microstructure, fracture surface fractography.

The problem of studying deformation of porous materials and their ductility is very important [1–3, 9] since it is connected with the extensive possibilities of hot forming (HF), primarily with preparation of complex shape components [9]. In this case porous material ductility presents increase specifications due to the impossibility of total avoidance of defects in the final HF stages that reduce strength properties. Information is available about the ductility properties of porous metallic materials [4–7] in a heated condition that makes it possible to develop rational HF technology for complex shape components. Selection of reliable criteria for plastic deformation resistance and failure is complicated by the influence if a large number of internal and external factors, and also the difficulty of performing prolonged tests at elevated temperature [8, 10, 11]. Solution of this problem requires a study of features of the composite material mechanical behavior drawing on defect theory that makes it possible to move from phenomenological and rough description of deformation and failure towards physically substantiated analysis of the atomic mechanism of these processes.

One of the main forms of tests making it possible to specify the most important material mechanical properties in an engineering respect is tensile testing.

At elevated temperatures and low stresses for creep (apart from internal slip) a special form of deformation is typical, i.e., grain boundary sliding. Deformation due to sliding may reach 20–30% of the overall deformation and consequently may make a marked contribution to the failure process. In contrast to low-temperature deformation with which ductile, transcrystalline (intersubgranular) failure is implemented, with grain boundary sliding (GBS) there is intercrystalline failure.

[1] Don State Technical University, Rostov-on-Don, Russia; e-mail: aquavdonsk@mail.ru.

[2] Don State Technical University, Rostov-on-Don, Russia; e-mail: rimmaruminskaya@gmail.com.

Translated from Metallurg, Vol. 65, No. 3, pp. 73–81, March, 2021. Original article submitted September 24, 2020.

 0026-0894/21/0304-0326

Table 1
Powder Chemical Properties and Preparation Method

Powder grade	Component weight fraction, %						Preparation method
	Mo	Ni	C	O	H	Cu	
Astaloy 85 Mo	0.85	–	0.02	0.09	–	–	Alloy steel powder atomization
Distaloy HP-1	1.5	4	0.01	–	0.1	2	Atomized powder diffusion alloying
ABC100.30	–	–	0.003	0.06	–	–	Molten iron atomization with high pressure water having good compaction capacity
NC100.24	–	–	0.02	–	0.14	–	Reduced iron powder from iron ore concentrate

A feature of many structural materials and alloys is presence of a descending section in nominal tensile diagrams connected with local plastic deformation within a neck formed before material failure. Specimen cross sectional area in the vicinity of neck formation decreases sharply, which is accompanied by a reduction in load required for subsequent specimen deformation before breakage. Correct analysis of the physical mechanisms of material plastic deformation and strengthening in the pre-failure stage requires determination of the σ–ε relationship corresponding to material reaction in a local area of a neck where plastic deformation is at a maximum and develops at the slowest rate. Consideration of just a reduction in cross section within a neck does not reflect the actual (true) material loading diagram within a local volume, since the distribution of plastic deformation within a neck is extremely non-uniform [12].

Iron powders produced overseas prepared by different technologies [10, 11] were used in the present work. Data for the overall chemical composition are provided in Table 1.

Astaloy 85 Mo powder, alloyed with 0.85% molybdenum, exhibits good compaction capacity and a uniform microstructure after sintering. These properties make it a distinguished material for preparing components with high hardness combined with good stiffness.

Distaloy HP-1 powder is based on Astaloy Mo grade powder that additionally contains 4% finely dispersed nickel powder and 2% copper powder.

NC100.24 powder is one of those used most extensively in the production of sintered components. An uneven particle surface and rough structure improves strength, and a low oxygen and carbon content provide a high degree of compaction capacity.

ABC100.30 powder has good compaction capacity. This capacity is especially considered in the production of high density components. A density up to 7.4 g/cm^3 is achieved in the course of one compaction operation.

Specimen dynamic breakage was performed in an Instron 1185 rupture machine with a force of 100 kN. The rupture machine has a muffle furnace that is fed with argon protective gas.

In order to test sintered specimens in tension specimens 4 mm in diameter according to GOST 1497 (Fig. 1) were machined from them. The breaking force was recorded by the rupture machine indicator. Specimens were heated from 900 to 1050 °C. Temperature was monitored by means of a chromel-alumel thermocouple, and the deformation rate was 2mm/min.

A failure surface was studied by electron microscopy by means of a ZEISS SUPRA 25 (Germany) universal laboratory scanning electron auto-emission microscope (Fig. 2). The microscope was adapted in order to resolve

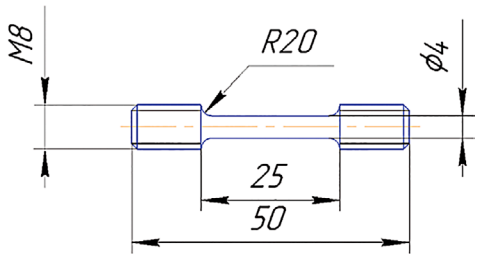

Fig. 1. Drawing of tensile test specimen.

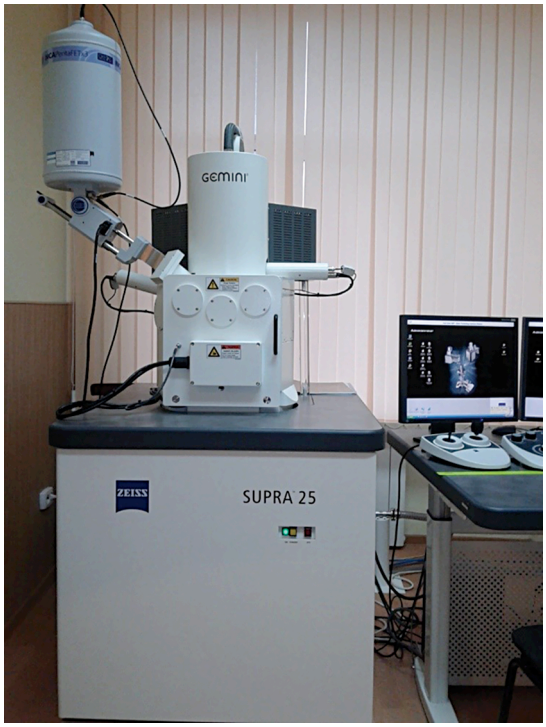

Fig. 2. ZEISS SUPRA 25 scanning electron microscope.

the problem over a wide range of applications: metallographic study of semiconductors, electron-beam lithography, observation of materials with small (nm) grain sizes, analysis of inclusions within alloy steels, analysis of fractures, and development of new materials and devices. It is intended for images of an object surface with high (up to 0.4 nm) spatial resolution, and also information about composition, structure, and other surface layer properties. Work is based on the principle of interaction of an electron beam with a test object. A contemporary scanning electron microscope (SEM) makes it possible to operate over a wide magnification range approximately up to $\times 1{,}000{,}000$, which exceeds by a factor of ≈ 500 the magnification of optical microscopes.

Performance of Experiments

Ultimate and yield strengths were determined in tensile tests with a deformation rate of 10^{-3} $\sec^{-1}$. Specimens after high-temperature tensile tests of powder materials are provided in Fig. 3. Test results are given in Table 2.

Fig. 3. Specimen after high-temperature breakage.

Table 2
Tensile Test Results for Cylindrical Specimens of Powder Material with Different Porosity (P = 10/20/30%) from Höganäs in Instron-1185 Universal Machine

Temperature T, °C	Specimen gauge length l_0, mm	Specimen number	$\sigma_{0.2} \pm 2.47$, MPa	$\sigma_f \pm 0.57$, MPa	$\delta \pm 0.67$, %	$\sigma_{0.2}/\sigma_f$
			Astaloy 85 Mo			
900	20	1.1	27/16/12	35/20/14	11.5/9/4.8	0.77/0.80/0.86
950	20	1.2	23/13/11	26/15/12	13.8/10/5.7	0.88/0.86/0.91
1000	20	1.3	20.5/11/9	24/13/10	15.9/12/6.5	0.85/0.84/0.9
1050	20	1.4	16/9/6.5	20/10/7	18.5/14/7.2	0.8/0.9/0.92
			Distaloy HP-1			
900	20	2.1	34/27/17	37/29/18	9.8/7/3.9	0.91/0.93/0.94
950	20	2.2	24/15/12.5	26/16/13	11/8.1/4.1	0.92/0.93/0.96
1000	20	2.3	21/13/11	25/14/12	14/10/5.5	0.84/0.92/0.92
1050	20	2.4	19/11/8.5	22/12/9	15/12.5/6	0.86/0.92/0.94
			ABC100.30			
900	20	3.1	16/10/7	22/13/9	18/15/10	0.72/0.76/0.77
950	20	3.2	14/9/6	20/12/7.5	20/15/12	0.7/0.75/0.8
1000	20	3.3	12/7/5	18/10/7	24/20.5/13	0.66/0.7/0.71
1050	20	3.4	10/6/5	16/8/7	28/22/14	0.62/0.7/0.71
			NC100.24			
900	20	4.1	21/13/10	25/14/11	14/13.5/7.5	0.84/0.92/0.9
950	20	4.2	20/12/9	24/14/10	16/13.5/8.5	0.83/0.85/0.9
1000	20	4.3	18/10/7	22/12/8	20/16/9	0.81/0.83/0.87
1050	20	4.4	15/8/6	19/10/7	24/18.5/10	0.78/0.8/0.85

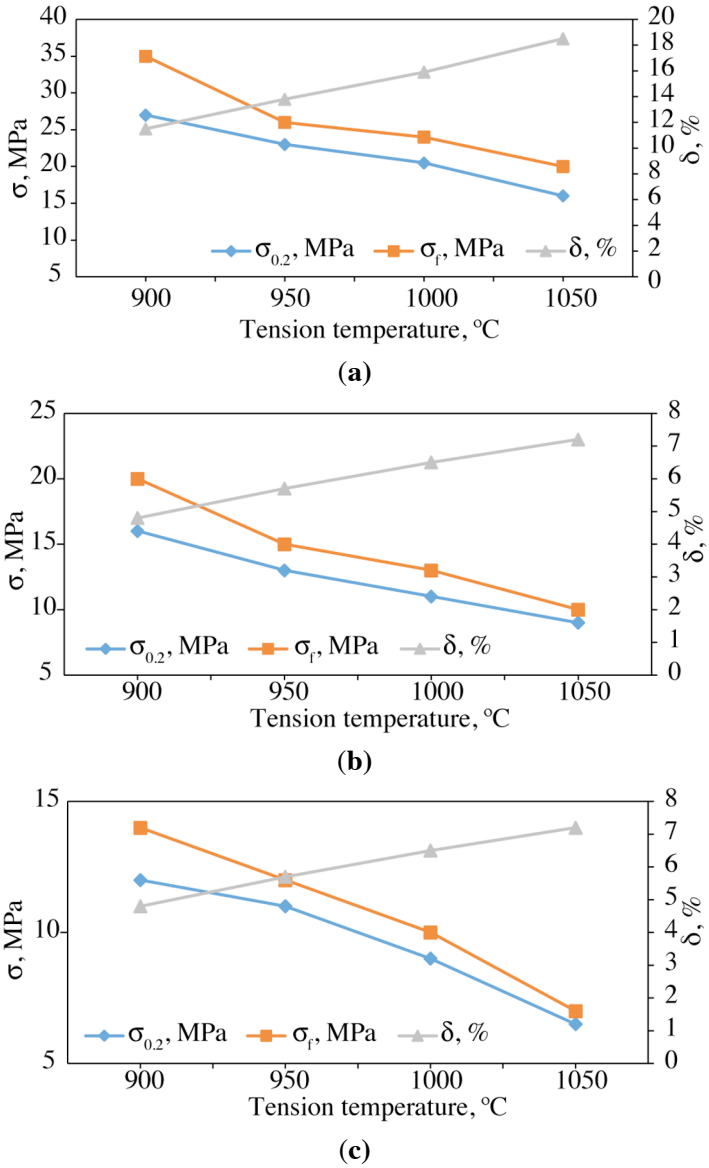

Fig. 4. Dependence of strength (σ_f, $\sigma_{0.2}$) and ductility (δ) properties on specimen tensile temperature for Astaloy Mo 85 grade material with initial porosity П: (a) 10%, (b) 20%, (c) 30%.

It is well known that with an increase in temperature there is a reduction in metal and alloy elastic properties. The effect of temperature on the level of strength and ductility properties is significantly more complex, especially for powder materials. Deformation involves metal strengthening. Temperature is a weakening factor, caused by phenomena of resting and recrystallization, and depending on temperature one of the factors may predominate (weakening or strengthening) increasing or reducing metal ductility [12, 13].

The effect of temperature on strength and ductility properties depends on the values of the powder material initial density, and also presence of impurities and alloying elements within the chemical composition (see Table 2) [14, 15].

With tension for specimens, apart from the main stresses causing porous material failure, within the stressed state scheme other (additional) stresses are absent. In view of this the limiting tensile deformation for a porous specimen was taken as an evaluation parameter for material ductility [16].

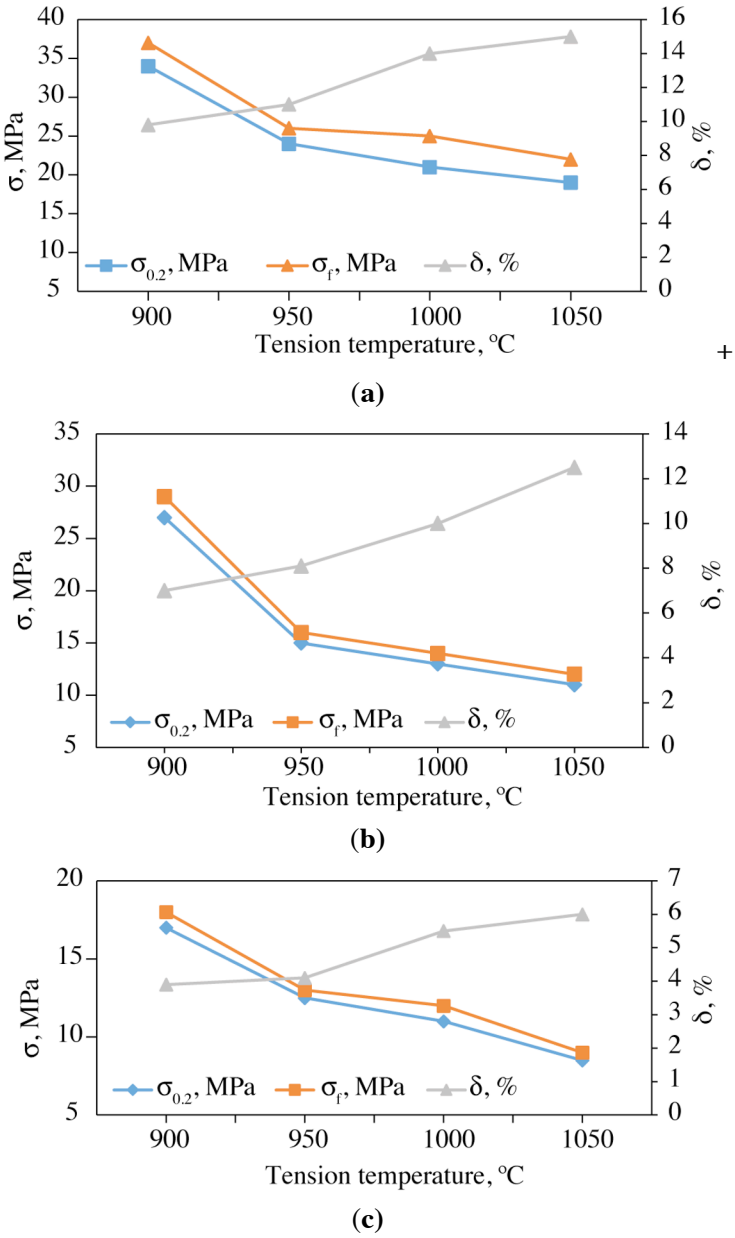

Fig. 5. Dependence of strength (σ_f, $\sigma_{0.2}$) and ductility (δ) properties on specimen tensile temperature for Distaloy HP-1 grade material with initial porosity П: (a) 10%, (b) 20%, (c) 30%.

Results of Experiments and Discussion

In this case in tension the concepts of "deformation capacity" (evaluated by the porous specimen tensile deformation limit) and "ductility" (expressing the capacity of porous material to deform plastically up to the start of failure under action of breaking stresses) coincide with respect to semantic value. For porous powder materials, having the same physical and mechanical properties, specimen deformation capacity is expressed in "limiting" tensile strains due to action of main and subsidiary stresses with identical production and test conditions, but different stress-strained state regimes, whereas ductility, expressed in "limiting "tensile strains due to action of breaking tensile stresses alone, should be identical and specify porous material physical properties.

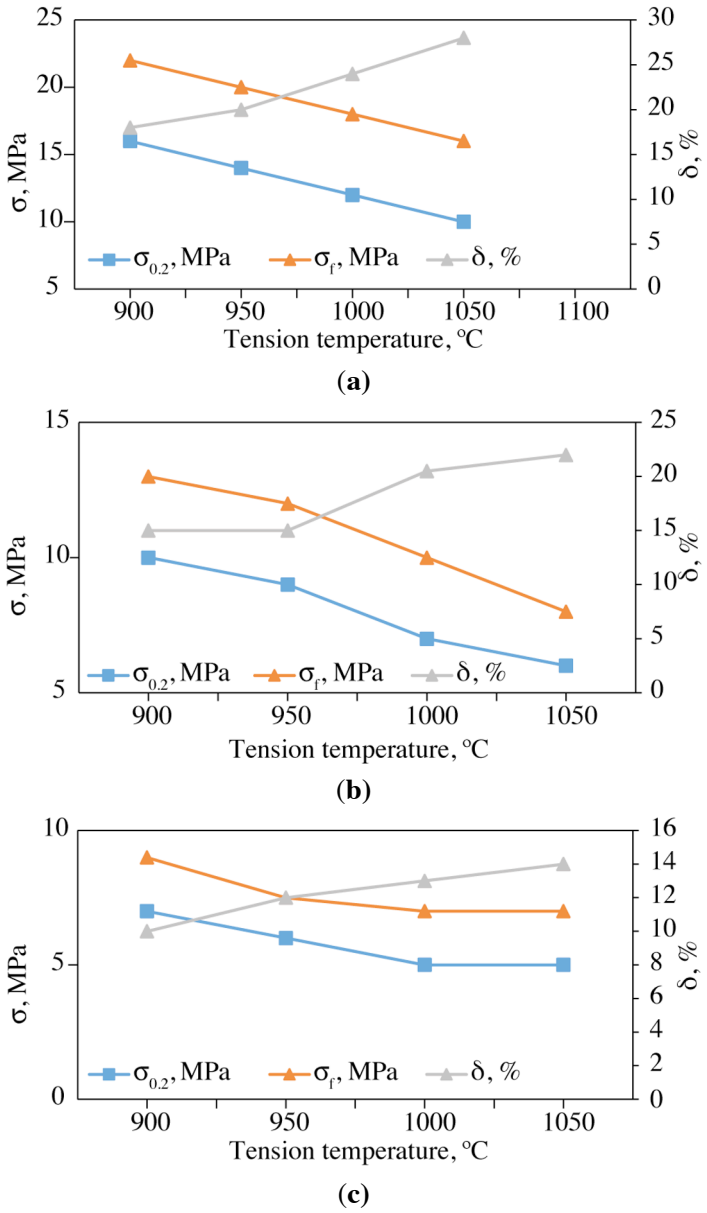

Fig. 6. Dependence of strength (σ_f, $\sigma_{0.2}$) and ductility (δ) properties on specimen tensile temperature for ABC100.30 grade material with initial porosity Π: (a) 10%, (b) 20%, (c) 30%.

Dependences for σ_f, $\sigma_{0.2}$, and δ on temperature for Astaloy 85 Mo powder material are given in Fig. 4, and show a uniform reduction in strength properties and an increase in ductility component with an increase in temperature. With $\Pi = 10\%$ relative elongation varies from 11.5 to 18.5%. With an increase in porosity the trend in test material behavior in relation to temperature is unchanged, although an apparent reduction in ultimate and yield strengths is observed. Values of relative elongation increase uniformly, pointing to a reduction in ductility properties with an increase in material porosity.

Changes in mechanical and ductility properties for material made from powder grade Distaloy HP-1 in the temperature range 950–1050 °C are provided in Fig. 5 with relationships whose nature is identical to those for material made from Astaloy 85 Mo grade material. However, the ultimate strength and plasticity are higher, but ductility properties are lower than in the case of Astaloy 85 Mo.

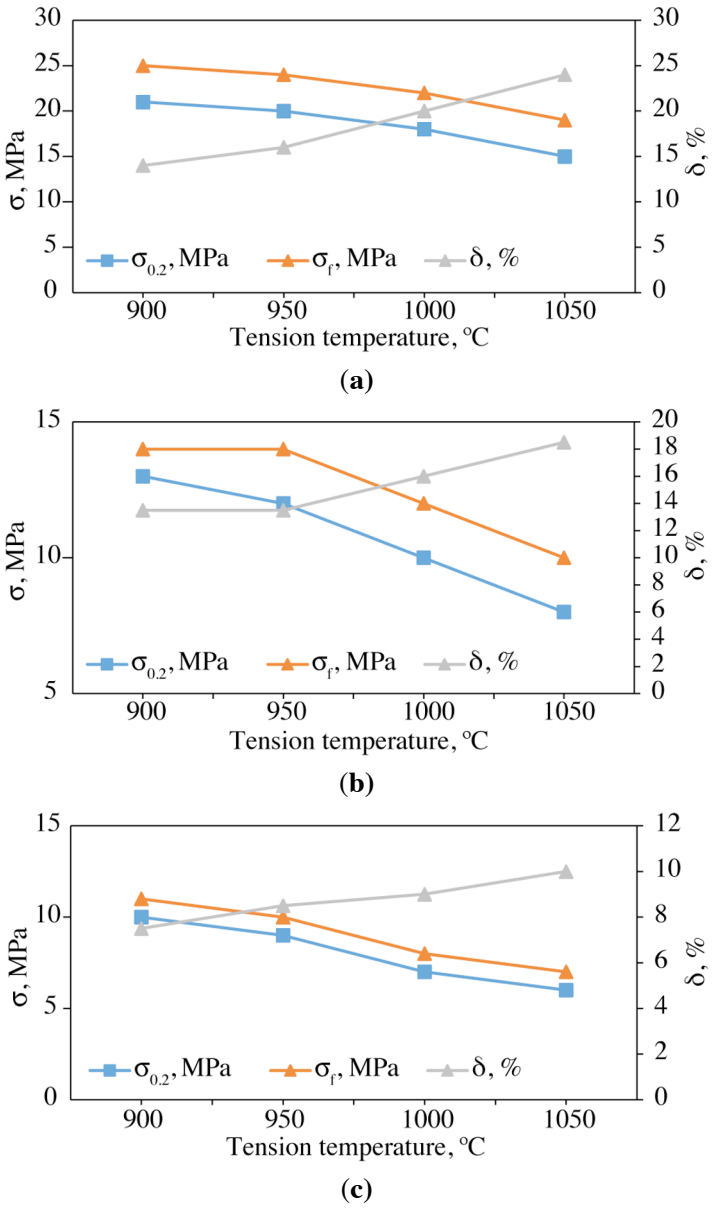

Fig. 7. Dependence of strength (σ_f, $\sigma_{0.2}$) and ductility (δ) properties on specimen breaking (tensile) temperature for NC100.24 grade material with initial porosity Π: (a) 10%, (b) 20%, (c) 30%.

The behavior of material made from powder grade ABC100.30 with an increase in temperature is characterized by the dependences given in Fig. 6, and points to the good ductility properties of the material with Π = 10% that makes it possible to conclude that use of this material is effective. On the whole dependences for σ_f, $\sigma_{0.2}$, and δ on temperature point to good ductility properties, i.e., 14–24%. Strength properties decrease uniformly with an increase in temperature, but ductility properties increase. Analysis of dependences points to the good ductility of material made from powder grade ABC100.30.

With a rupture temperature of 900 °C for specimens made from material grade Distaloy HP-1 a very high value is recorded for yield strength of $\sigma_{0.2}$ = 34 MPa (see Fig. 5a) compared with specimens made from materials Astaloy 85 Mo, ABC100.30, and NC100.24. This is explained by the larger amount of alloying elements and

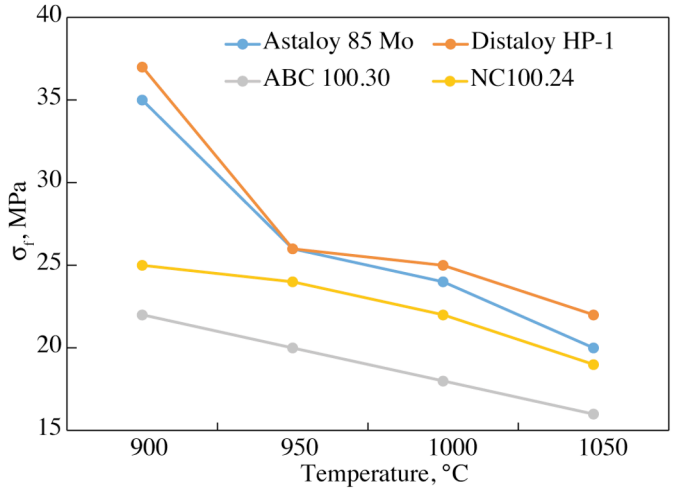

(a)

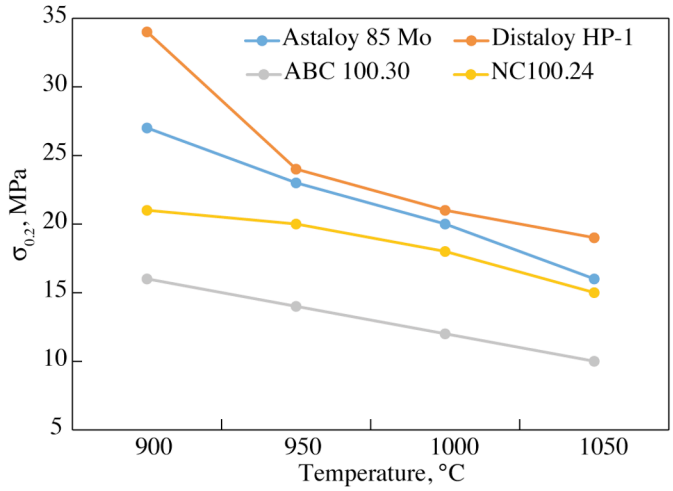

(b)

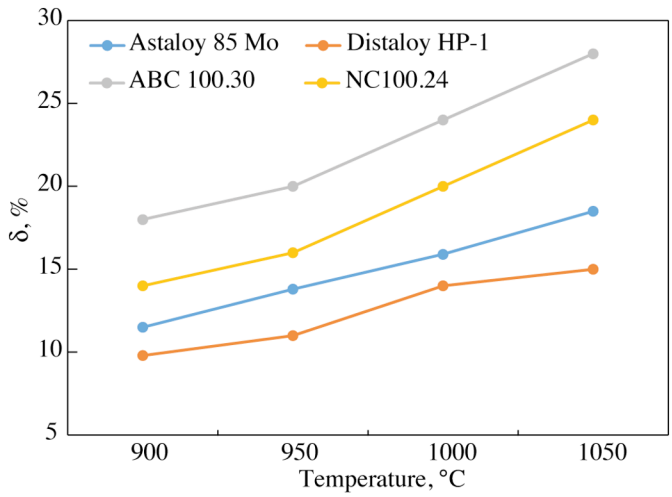

(c)

Fig. 8. Dependence of ultimate strength (a), yield strength (b), and relative elongation (c) on temperature for Astaloy 85 Mo, Distaloy HP-1, ABC100.30, and NC100.24 materials with porosity $\Pi = 10\%$.

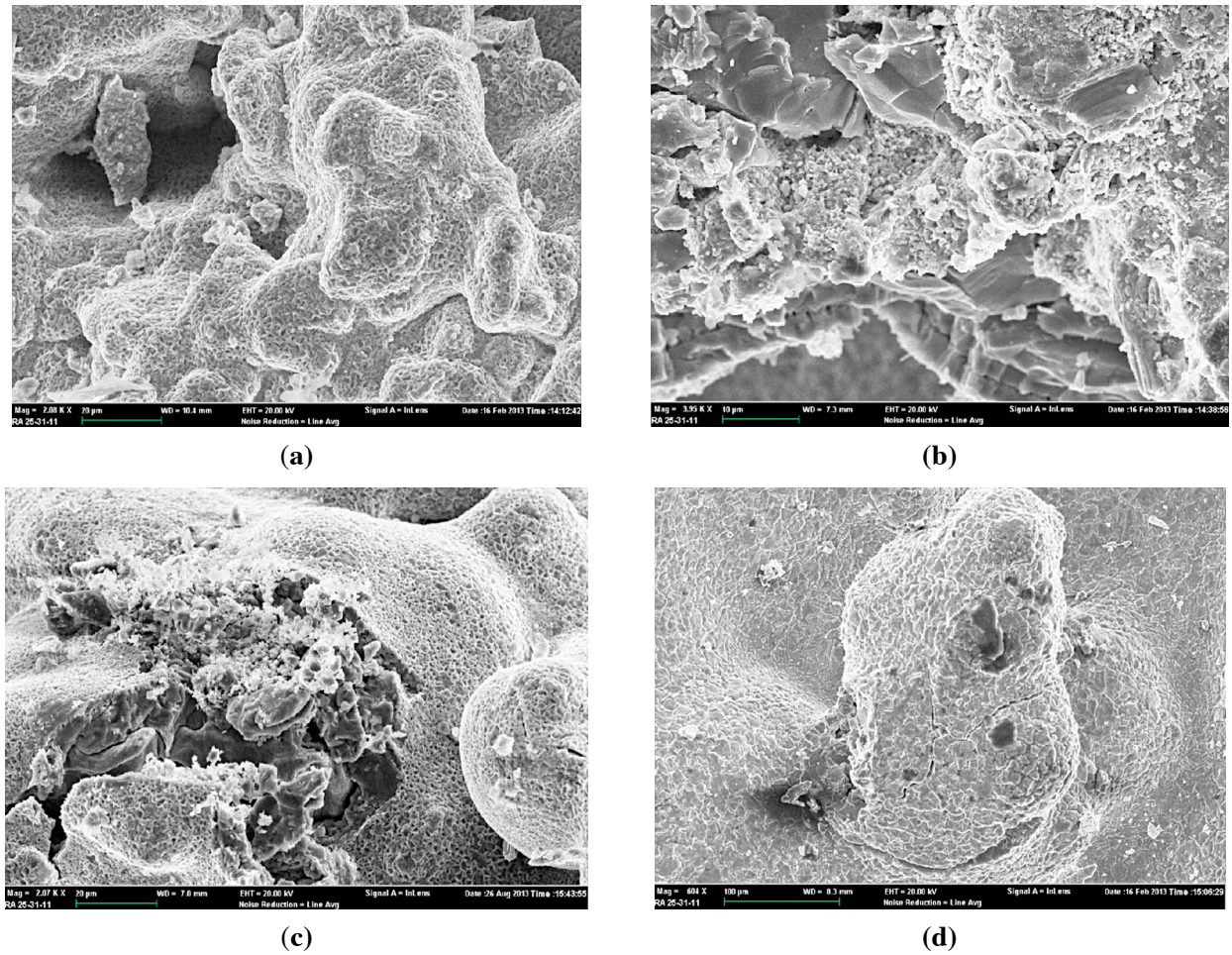

Fig. 9. Astaloy 85 Mo powder material failure surface (Π = 10%) after high-temperature tension, $\times 10^6$: (a) 900 °C, (b) 950 °C, (c) 1000 °C, (d) 1050 °C.

the greater their percentage content the higher is material strength. With an increase in the strength of materials Distaloy HP-1 and Astaloy 85 Mo their ductility properties are lower than those for materials of powder grades ABC100.30 and NC100.24 (Fig. 7).

Tests have demonstrated that with an increase in temperature there is a reduction in plastic deformation resistance, and ultimate strength correlates with crack formation (Fig. 8). The best ductility properties are exhibited by material made from alloy grade ABC100.30 (see Fig. 8c), and the best strength properties are exhibited by specimens made from alloy grade Distaloy HP-1 (see Fig. 8a, b).

Brittle and quasibrittle forms of failure are observed for material of specimens whose tension was conducted at 900 °C. Tension at higher temperature has ductile and quasiductile failure [13, 17–20].

Fracture Surface Electron Microscopy

Failure during high-temperature strength tests often arise by micropore generation at the junction of grain boundaries as a result of developing grain-boundary sliding or local melting [12, 17–19].

Subsequent diffusion of vacancies or development of local slip may increase pores to the size of microcracks (Fig. 9a, b), which propagate along grain boundaries causing intergranular cracking. Splitting is observed along

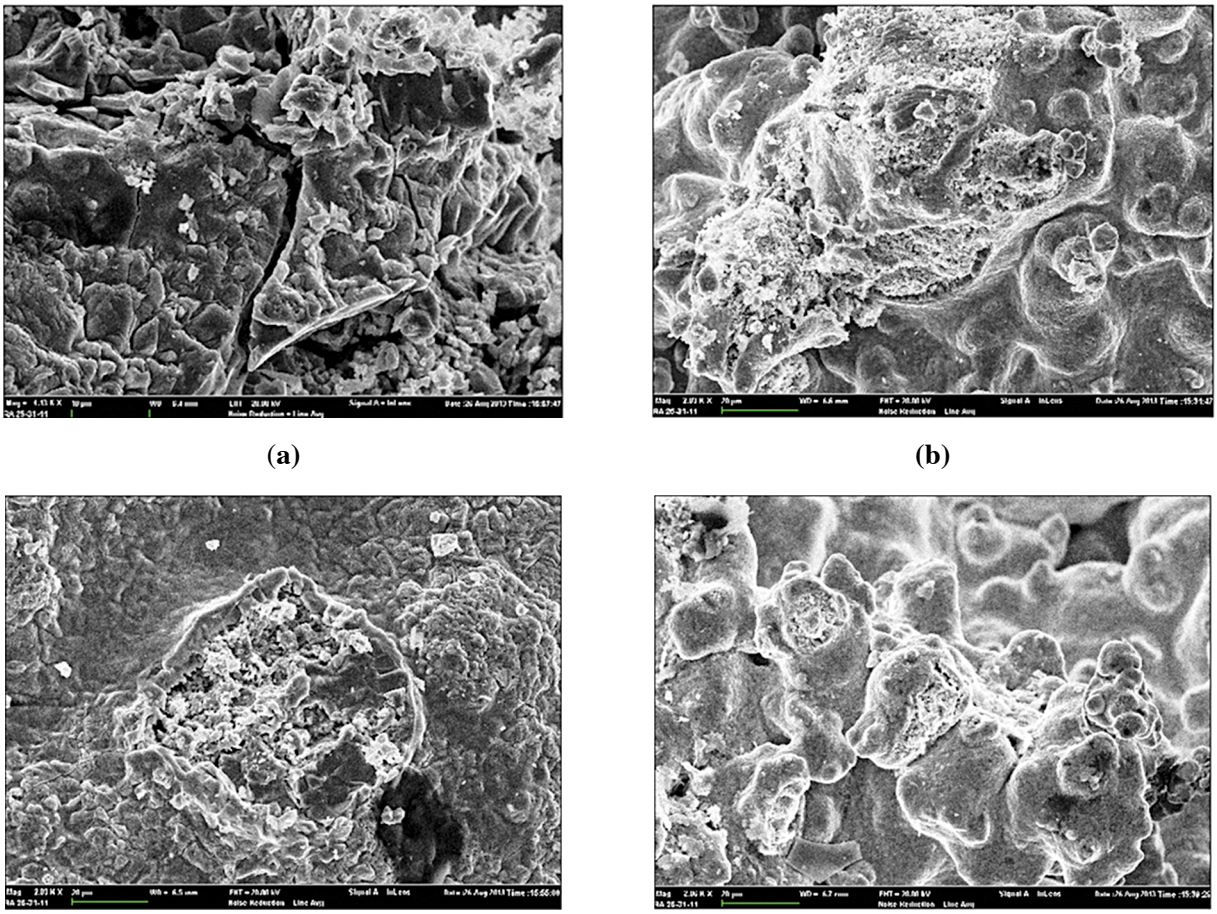

Fig. 10. Distaloy HP-1 powder material failure surface (Π = 10%) after high-temperature tension, $\times 10^6$: (a) 900 °C, (b) 950 °C, (c) 1000 °C, (d) 1050 °C.

grain boundaries, grains are extended, and their edges are rounded. Flat smooth facets inherent for intergranular failure at room temperature were observed within grains. Signs of oxidation were seen at the surface of grain that arise at elevated temperature after final failure.

Exposure of certain materials containing Mo, Ni, Cu, at high temperature may lead to embrittlement and subsequent intergranular failure as a result internal oxidation over grain boundaries that is demonstrated in Fig. 10.

Grain boundaries are modified as a result of formation of copper and nickel oxides; failure propagated through a brittle oxide layer. As a result during failure of Distaloy HP-1 at 900 °C (see Fig. 10) the cyclic nature of crack propagation is observed that is indicated by a number of micro-channels similar to those observed during fatigue. Subsequent continuous failure of a microstructure previously embrittled with oxides may lead to formation of intergranular facets somewhat different in form due to layers of oxides and deformation lines connected with plastic deformation during final rapid failure.

With a certain combination of temperature, stress, and test material at the surface of grain boundaries there may be complex reliefs in the form of pores and elevations with typical stepped facets merging into each other. Test material ABC100.30 during high-temperature failure is the most ductile, which is illustrated by SEM pictures in the form or rounded grain outlines (Fig. 11).

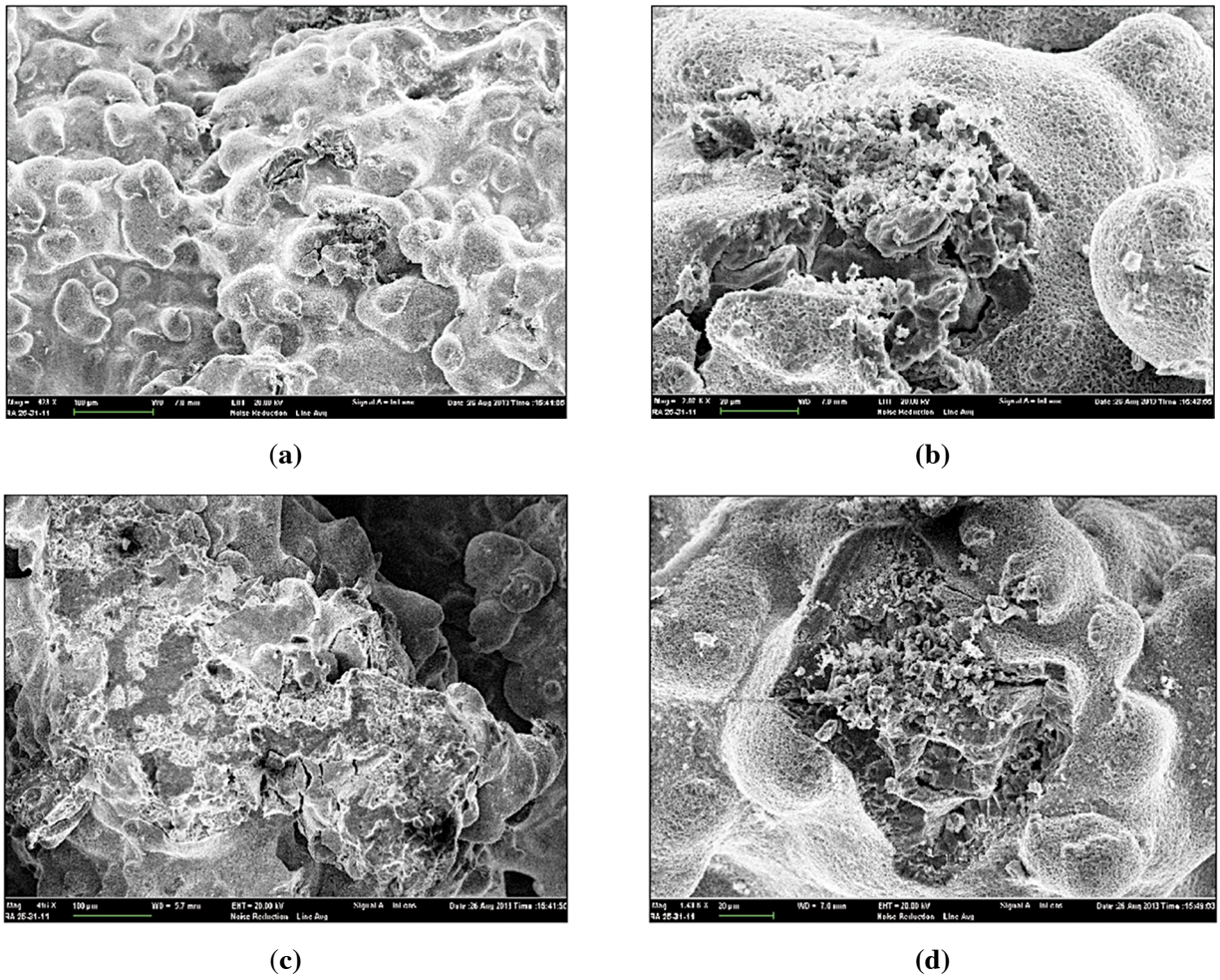

Fig. 11. ABC100.30 powder material failure surface (Π = 10%) after high-temperature tension, $\times 10^6$: (a) 900 °C, (b) 950 °C, (c) 1000 °C, (d) 1050 °C.

Fractograms representing the failure surface of material NC100.24 in the test temperature range indicate that with an increase in rupture temperature the ductility properties increase. In Fig. 12 the feature established is observed at a fracture surface: grains are extended and have a rounded outline expressed most clearly with an increase in temperature.

CONCLUSIONS

1. Morphological differences have been revealed for the structure of central and peripheral areas of material. The latter are characterized by greater difference in grain size and increase micropore concentration, directionality of micropore and nonmetal inclusion accumulations along previous boundaries of powder particle physical separation.

2. Fractographic study of powder materials has made it possible to reveal areas of fractures having different relief at intercrystalline shears over their whole extent, which points to presence of areas at a contact surface between particles of a different degree of consolidation perfection.

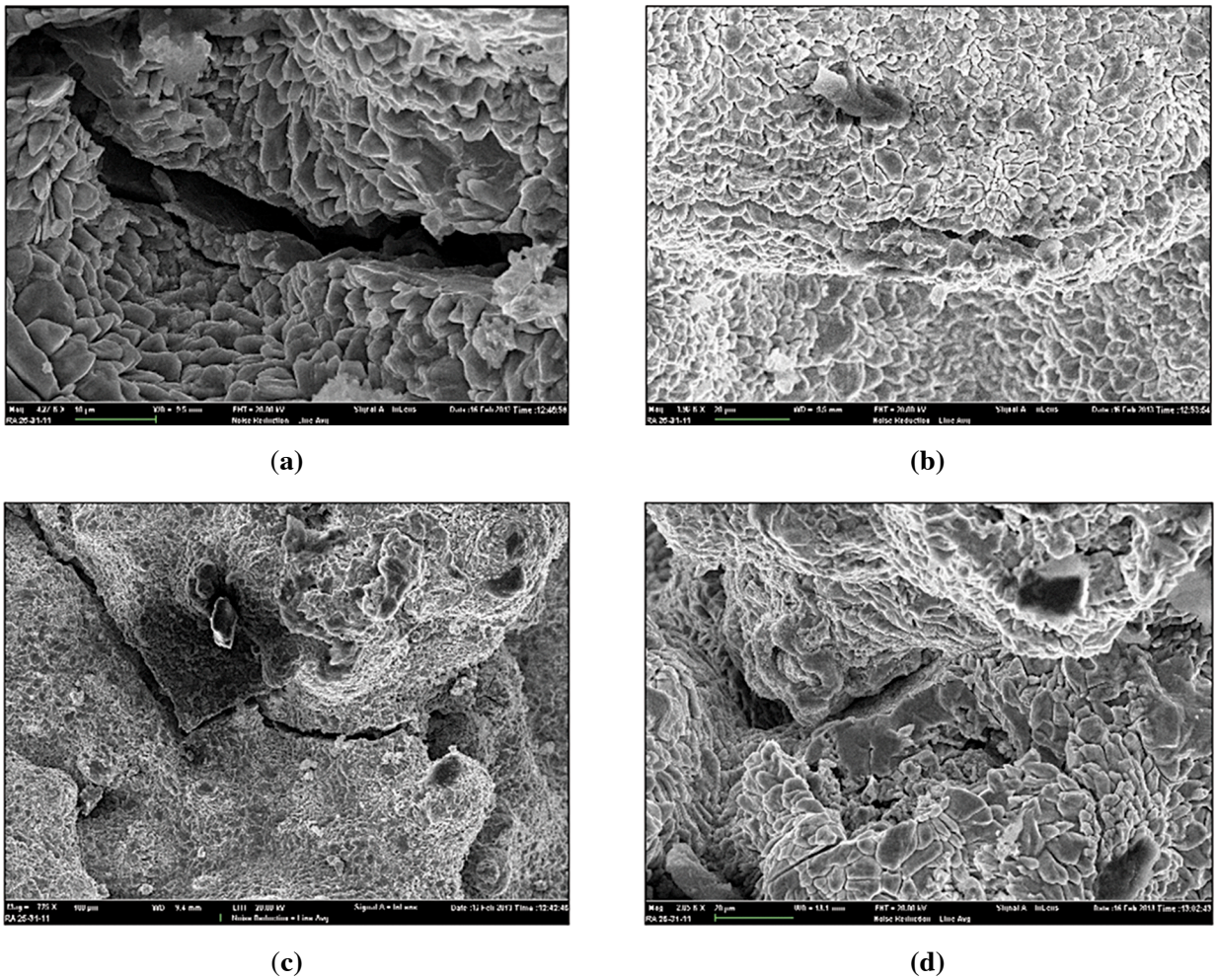

Fig. 12. NC100.24 po`wder material failure surface (Π = 10%) after high-temperature tension, $\times 10^6$: (a) 900°C, (b) 950°C, (c) 1000°C, (d) 1050°C.

3. It has been established that plastic flow is accompanied by formation of the peripheral area structure whose structure and properties depend on the degree of deformation and production conditions. As a peripheral area develops, a reduction is observed in material strength properties after reaching a critical value for transverse flow [17–20].

REFERENCES

1. Yu. G. Dorofeev, *Dynamic Hot Compaction of Porous Powder Workpieces* [in Russian], Metallurgiya, Moscow (1977).
2. Yu. G. Dorofeev, L. G. Marinenko, and V. I. Ustimenko, *Structural Power Materials and Objects* [in Russian], Metallurgiya, Moscow (1986).
3. G. A. Baglyuk, "Analysis of the kinematics of a porous cylinder free upsetting taking account of contact friction," *Poroshk. Metall.*, No. 1, 17–21 (1993).
4. V. V. Sinel'shchikov and A. S. Razymnyi, "Evaluation of porous material ductility in a heated condition for specimen free upsetting," *Powder and Composite Materials and Objects, coll. work*, YuRGTU, Cherkassk (2005).
5. V. V. Sinel'shchikov, S. N. Egorov, and Yu. V. Dybov, "Study of features of failure of growth zones of heated porous material with uniaxial tension," *Progressive Technology of Engineering Systems: Proc. V Internat. Sci. Tech. Conf. "Engineering and Technosphere Abroad of the XXI Century" (Sevastopol', 8–11 September 1998)*, DonGTYu, Donetsk (1998).

6. E. Robert-Perron, C. Blais, and S. Pelletier, "Tensile properties of sinter hardened powder metallurgy components machined in their green state," *Powder Metallurgy*, **52**, No. 1, 80–83 (2009).
7. V. N. Antsiferova, *Problems of Contemporary Materials and Technology* [in Russian], Perm. Gos. Tekh. Univ, Perm' (1995).
8. Yu. G, Gurevich, V. N. Antsiferov, L. M. Savinykh, S. A. Oglezneva, and V. Ya. Bulanov, *Wear Resistance of Composite Materials* [in Russian], UrO RAN, Ekaterinberg (2005).
9. V. Yu. Dorofeev and Yu. G. Dorofeev, "Stamping of powder workpieces: today and tomorrow," *Poroshk. Metall*., No. 7/8, 27–36 (2013).
10. M. S. Egorov, R. V. Egorova, V. N. Pustovoit, and A. A. Atrokhov, "Mechanical properties of powder materials after free upsetting," *Metallurg*, No. 3, 93–96 (2020).
11. V. Yu. Dorofeev and S. N. Egorov, *Particle Growth During Formation of Powder Hot-Deformed Materials* [in Russian], Metallurgizdat, Moscow (2003).
12. A. K. Grigor'ev and A. I. Rudskoi, *Powder Material Deformation and Compaction* [in Russian], Metallurgiya, Moscow (2002).
13. G. A. Baglyuk, "Comparative analysis of the deformed state of porous workpieces during stamping in closed and open dies," *Obrab. Metall. Davleniem*, No. 2, 147–153 (2012).
14. M. B. Shtern and E. V. Kartuzov, "Features of the occurrence of propagation and impact waves in highly porous materials," *Poroshk. Metall.,* No. 3, 13–22 (2016).
15. Zh. V. Eremeeva, N. M. Nikitin, N. P. Korobov, and Yu. S. Ter-Vaganyants, "Study of treatment of powder steels alloyed with anno-size additions," *Nanotekhnol: Nauka Proizvod*., No. 1(38), 63–74 (2016).
16. M. S. Egorov and S. N. Egorov, "Hot-deformed low-alloy structural steels," RF Ministry of Education and Science, Federal Agency for Education, YuRGTU (Novocherkassk Politech. Inst.), Novocherkassk (2008).
17. R. V. Egorova, "Microstructural analysis of a stepped shape surface," *Metallurg*, No. 6, 65–67 (2009).
18. A. A. Mamonova, "Features of fine crystalline structure formation and optimization of powder steel stamping processes," *Author's Abstr. Cand. Techn. Sci*., Kiev (2007).
19. M. S. Egorov, and R. V. Egorova, "Ductility of composite materials with determination of hot stamping regimes excluding defect formation within the material structure," *Zagotvit. Proizvod. Mashin*., **17**, No. 2, 66–72 (2019).
20. A. A. Glotka and A. N. Moroz, "Comparative effect of carbides and nonmetallic inclusions on microcrack formation within steels," *Metalloved. Term. Obrab. Materialov*, No. 8, 61–65 (2019).